ELSEVIER

Catalysis Today 33 (1997) 73-83

CATALYSIS TODAY

Partial oxidation of methane to formaldehyde on silica-supported transition metal oxide catalysts

M.A. Bañares, L.J. Alemany, M. López Granados, M. Faraldos, J.L.G. Fierro *

Instituto de Catálisis y Petroleoquímica, CSIC, Campus UAM, Cantoblanco, 28049 Madrid, Spain

Abstract

This work describes the partial oxidation of methane on high surface area silica-supported redox oxide catalysts (MO_x/SiO_2; M = V, Mo, W and Re). Formaldehyde, C_2H_n, and CO_2 are primary products obtained in this reaction, while CO originates from further oxidation of formaldehyde and hydrocarbons. Supported vanadium oxide was found to be the most reactive due to its higher reducibility, thus providing additional sites for oxygen activation. Rhenium oxide exhibited high specific activity and selectivity, however it deactivates from sublimation of metal oxide under on-stream operation at high temperatures, typically above 773 K. Results suggest a reaction scheme where oxygenates and oxygen-free intermediates are present yielding HCHO, CO_x and C_2H_n hydrocarbons.

Keywords: Partial oxidation; Methane; Formaldehyde; Silica-supported transition metal oxide catalysts

1. Introduction

The partial oxidation of methane (POM) with oxygen to C_1-oxygenates has been widely investigated in the last decade [1–8]. Most of the studies using redox type (Mo, V) oxide catalysts have concentrated on the reaction mechanism [9–12] and structure–selectivity relationships [13–15]. The similarity of the active phases and preparation procedures is a common characteristic to all these catalysts [16–19] and no clear correlation has been proposed to account for the different catalytic performance on catalytic selective oxidation of methane to C_1-oxygenates.

Tracer isotopic studies [9,12] on silica-supported molybdenum oxide catalysts with $^{18}O_2$ present evidence that the oxygen incorporated in to the molecule of methane comes from lattice oxygen and not from gas phase molecular oxygen. The role of oxygen (the most common oxidant) appears to be related to reoxidation of the catalysts [20]. However, the role of oxygen also appears to be related to the initial activation of the methane molecule, as isotopic studies [10] and homogenous vs. heterogeneous reaction suggest [21]. The role of oxygen for initiation of the reaction appears to be related to its ability to generate methyl radicals, as evidenced by the remarkable increase of reactivity observed by increasing the methane–oxygen mixing volume at a reaction temperature [21]. The use of chemical radical initiators has a similar effect [22,23] and the use of $CH_4 + O_2$ mixing volume with radical initiators increases outstandingly its reactivity. In the absence of

* Corresponding author. (FAX: +34-1-585-4760; E-mail JL-GFIERRO@ICP.CSIC.ES).

PII S0920-5861(96)00099-5

methane–oxygen mixing volume and radical initiators no gas phase activation of methane is expected leaving the catalyst alone to activate methane since the void volume between the particles is too small to allow a significant activation of methane. No, or few, methane conversion is recorded in the absence of molecular oxygen [10]. Methane is not activated by the catalyst alone; oxygen is the key to activate methane. It can be expected that oxygen is activated on the surface of the catalyst, thus enabling methane activation. Consequently, the study of methane conversion is the study of oxygen activation [10].

The aim of this work is to provide a fundamental knowledge on simple silica-supported metal oxides to evaluate the behavior of different individual oxides prior to the study of multicomponent catalysts. Silica-supported oxides may present different structures, depending on their surface loading [24]. The activity for methane conversion has been reported to be related to dispersed isolated surface metal oxides on silica-supported molybdenum and vanadium oxides [11,14,15,22,25]. These structures are observed below a surface loading of about 1 atom per nm^2 of silica support. Consequently, we have prepared four different dispersed silica-supported metal oxides (MO_x/SiO_2; M = V, Mo, W and Re) and tested them for the selective oxidation of methane. Tungsten has also been selected for this study due to the similarity of redox properties between WO_3 and MoO_3. Rhenium oxide has been chosen due to its high reactivity to activate C–H and C–C bonds [26–29].

2. Experimental

2.1. Catalyst preparation

A non-porous silica Degussa Aerosil-200 (ca. 200 m^2/g) was used as the support for all catalysts studied. MoO_3/SiO_2 was prepared by aqueous impregnation of ammonium heptamolybdate (Merck, reagent grade) in a rotary evaporator. The impregnate was dried at 393 K overnight and calcined at 923 K for 5 h. V_2O_5/SiO_2 was prepared by impregnation of silica in a similar manner by an aqueous solution of ammonium metavanadate (Merck, reagent grade) solubilized by hydrogen peroxide. Drying and calcination were accomplished as described above. WO_3/SiO_2 samples were prepared by two methods: (i) aqueous impregnation in a rotary evaporator of ammonium metatungstate (Fluka, reagent grade), and (ii) impregnation by a methanol–ethanol solution of WCl_6 (Fluka, reagent grade). In both procedures drying and calcination were done as above. Re_2O_7/SiO_2 was prepared by aqueous impregnation of perrhenic acid (Aldrich, reagent grade) in a rotary evaporator. Samples were dried at 393 K overnight. Due to the high volatility of supported rhenium oxide [30,31], special care was taken in this catalyst to minimize rhenium oxide losses by sublimation. V, Mo, and W catalysts were prepared to have a nominal surface coverage of 0.8 metal atoms per nm^2 of silica support. For the sake of simplicity, they will be referred to 0.8 V, 0.8 Mo, and 0.8 W. The exception was silica-supported rhenium oxide which was prepared for a coverage of 0.05 Re atoms per nm^2 of silica support (0.05 Re), in order to minimize as much as possible oxide loss by volatilization. Samples prepared with a rhenium surface coverage as low as 0.5 Re atoms per nm^2 of silica support resulted in very significant volatilization of rhenium, as evidenced by a mirror formed on the walls of the reactor downstream from the bed of the catalyst. All catalysts were sieved to a particle size range 0.12–0.25 mm.

2.2. Catalyst characterization

Raman spectra were recorded with a Brucker FT Raman instrument using a 1064 nm excitation line. Samples were placed in a stationary sample holder under ambient conditions. The power measured at the sample was ca. 40 mW.

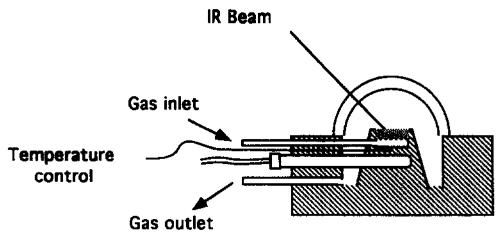

Fig. 1. Schematic view of the infrared diffuse reflectance reaction cell (DRIFTS).

TPR experiments were recorded on a Micromeritics equipment model TPR/TPD-2900 fitted with a TCD detector and controlled by a computer. Samples of 25 mg were used. The sample was pre-treated at 423 K in helium for 1 h. TPR experiments were run in a 10% H_2/Ar stream heating the sample up to 1273 K at a rate of 10 K/min. The infrared spectra were recorded on very thin self-supporting wafers (8–10 mg cm^{-2}) of samples placed in a special infrared cell assembled with greaseless stopcocks and KBr windows, which allowed catalyst pretreatments either in a vacuum or in a controlled atmosphere (Fig. 1). The samples were first purged with a He flow while heating up to 773 K, then reduced in a H_2 flow (60 cm^3 min^{-1}) at this temperature for 1 h. After reduction, the catalysts were outgassed under a high vacuum for 0.5 h and then cooled down to room temperature. Next they were exposed to 4 kN m^{-2} NO and the infrared spectra were recorded on a Nicolet ZDX Fourier transform spectrophotometer. Photoelectron spectra were acquired with a Fisons ESCALAB 200R spectrometer equipped with a hemispherical electron analyzer and an MgK_α X-ray exciting source (1253.6 eV). The samples were mounted on a sample rod placed in a pretreatment chamber and outgassed under vacuum prior to transfer into the analysis chamber. The pressure in the ion-pumped analysis chamber was below 3×10^{-9} Torr during data acquisition. The C 1s, O 1s, Si 2p, Mo 3d, W 4f, Re 4f, and V 2p peaks were recorded. The intensities were estimated by calculating the integral of each peak after subtraction of the 'S' shaped background and fitting the experimental curve to a mixture of Lorentzian and Gaussian lines of variable proportion [32]. The binding energies were calculated using the Si 2p peak at 103.4 eV and the C 1s peak at 284.9 eV. The accuracy of the BE values was within ± 0.2 eV.

To obtain further insight into the behavior of adsorbed intermediates, the 0.8 V catalyst was impregnated with HCHO in a solution of water and methanol. Studies of the evolution of adsorbed formaldehyde were performed using an in situ DRIFTS cell (Harrick Co., model reaction chamber HVC DR3) in flowing oxygen. Samples were placed (particle size < 0.12 mm) on the sample cup. Gases pass into the cell through the sample bed, and its temperature is controlled by a heating cartridge close to the sample holder. Further information on the species evolving from the surface of the catalyst can be obtained from temperature programmed reaction-mass spectrometry using a Balzers quadrupole mass spectrometer QMG 125. Evolution of evolving species could be monitored by recording the m/e signals of CH_4, CH_3OH, HCHO, C_2H_6, CO, H_2O, and CO_2 species. The catalyst was heated from 298 to 873 K (5 K/min) in vacuum.

2.3. Catalytic test

Activity measurements were carried out at atmospheric pressure in a fixed bed quartz microcatalytic reactor by co-feeding CH_4 (99.95 vol%) and O_2 (99.98 vol%) without diluent. The CH_4:O_2 molar ratio was adjusted to 2 by means of mass flow controllers, and the methane residence time was adjusted to 2 g h mol^{-1}. Catalyst loading was 50 mg and it was sieved to the particle size range of 0.12–0.25 mm. The reactor effluent was analyzed by an on-line Hewlett Packard HP-5890-II gas chromatograph fitted with thermal conductivity detector. Chromosorb 107 and 5A molecular sieves packed columns were used with a column isolation analysis system.

3. Results

FT-Raman shows the absence of sharp Raman bands characteristic of crystalline structures on fresh and used 0.8 Mo, 0.05 Re and 0.8 V catalysts. No Raman bands could be recorded from the dispersed surface oxides due to the low sensitivity of FT-Raman to these species. Raman spectra of the 0.8 W catalyst prepared by impregnation in aqueous solution of ammonium metatungstate shows sharp Raman bands at 807, 715, and 272 cm^{-1}, characteristic of crystalline WO_3 (Fig. 2). Crystalline WO_3 was obtained even at the lowest tungsten oxide loading attempted. Consequently, an alternative preparation method was used by impregnation on silica of a methanol–isopropanol solution of WCl_6. This preparation did not show bands of crystalline WO_3. Only a broad feature at ca. 800 cm^{-1} might be indicative of a weak aggregation of the tungsten oxide species. The importance of tungsten oxide precursor on the nature of silica-supported W(VI) has recently been reported [33]. Since surface dispersed oxide species are more active for methane conversion, only the better dispersed WO_3/SiO_2 catalysts has been used in this study.

TPR profiles are presented in Fig. 3. No TPR profile is presented for the rhenium catalyst due to its extremely low loading. Hydrogen consumption starts at very low temperatures for silica-supported vanadium oxide catalysts (480 K) reaching a maximum at about 775 K. The 0.8 Mo catalyst presents two reduction stages at about 744 and 914 K. Very low hydrogen consumption is observed at a lower temperatures. Silica-supported tungsten oxide presents a single reduction maximum at about 881 K. Reduction of this oxide at lower temperatures is negligible.

NO chemisorption on catalysts pre-reduced at 773 K are presented in Fig. 4. Silica-supported

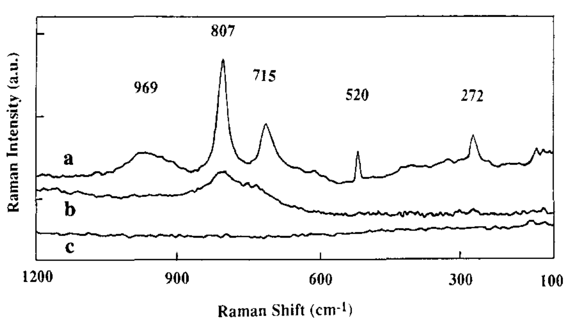

Fig. 2. Ambient FT-Raman spectra of 0.8 W catalysts prepared by impregnation with ammonium metatungstate (a); prepared by impregnation of WCl_6 in ethanol–isopropanol solution (b); and on silica support (c).

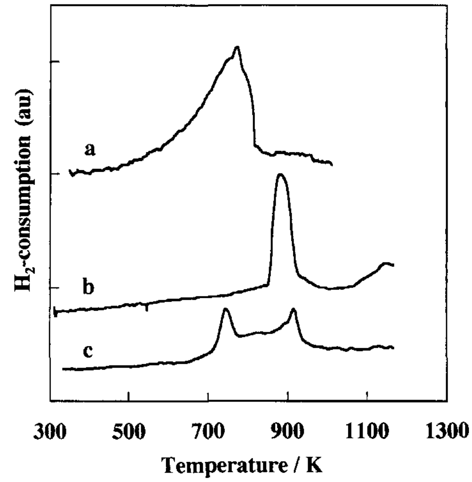

Fig. 3. Temperature-programmed reduction profiles of different catalysts: (a), 0.8 V; (b), 0.8 W; and (c), 0.8 Mo.

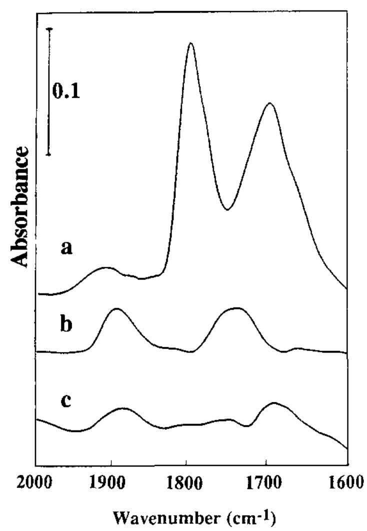

Fig. 4. IR spectra of NO chemisorbed on pre-reduced catalysts by hydrogen at 773 K: (a), 0.8 Mo; (b), 0.8 V; and (c) 0.8 W.

Table 1
IR and XPS data of silica-supported oxide catalysts

Catalyst	NO chemisorption		$(Metal/Si)_{XPS}$	
	Fresh	Used	Fresh	Used
0.8 V	2.0	0.9	0.050	0.015
0.8 Mo	17.2	21.9	0.061	0.069
0.8 W	0.8		0.063	0.060
0.05 Re			0.019	0.005

molybdenum, vanadium and tungsten oxides exhibit two IR bands of NO adsorbed as dimeric (or dinitrosyl) species on reduced sites. The intensity of the NO absorption is much higher in the 0.8 Mo catalyst than on its 0.8 V counterpart. The degree of reduction of metal oxide determines to a great extent the number of adsorption sites and hence the NO surface concentration. Thus, while molybdenum oxide is essentially reduced to Mo^{4+} [15], dispersed vanadium oxide is reduced to V^{3+} rather than to V^{4+} [15,34]. NO adsorption on tungsten oxide catalysts is very low, which is consistent with the very low degree of reduction of this catalyst at 773 K (cf. Fig. 3b).

Comparison of NO adsorbed on 0.8 Mo and 0.8 V catalysts shows some interesting differences after catalytic tests (Table 1). The amount of chemisorbed NO on 0.8 Mo is not significantly altered by reaction conditions. That is not the case for 0.8 V where the NO chemisorption band decreases markedly. Previous laser Raman characterization of these materials showed that the 0.8 V catalyst presents a weak aggregation as V_2O_5 crystallites as evidenced by weak features at ca. 990 and 270 cm^{-1} [15]. The presence of vanadia micro crystals has also been observed in other vanadia/silica materials with equivalent surface vanadium oxide coverage (5% V_2O_5 on fumed Cab-O-Sil Cabot EH-5 silica, 380 m^2 g^{-1}, i.e. 0.85 V atoms per nm^2 of silica support) [35]. Since the selective oxidation of methane is performed at temperatures above 850 K, significant volatilization of aggregated vanadia is expected [36], thus decreasing the extent of chemisorbed NO. Photoelectron spectroscopy was used to further evaluate the stability of the silica supported oxides. The metal to silicon XPS atomic ratios are presented in Table 1. No significant changes could be recorded on the values for molybdena/silica and tungsta/silica samples. Conversely, the parent 0.8 V sample exhibits a loss of vanadium oxide species. The decrease of V/Si XPS ratio can not be due to aggregation of vanadium into crystallites since their formation is not observed by Raman spectroscopy of the used sample. The same trend is observed for the silica-supported rhenium oxide. Loss of the rhenium oxide phase has previously been observed on supported rhenium oxides [31,37] and is due to the fact that Re_2O_7 sublimates at temperatures as low as 475 K [38]. The use of silica support strongly limits the amount of stable supported rhenium oxide due to its very low capacity to disperse oxides [39,40] as compared to other supports like alumina, titania, magnesia, etc. Silica-supported oxides (Re, V, Cr, Mo, etc.) in the presence of an admixed oxide support (TiO_2, Al_2O_3, etc.) migrate to the admixed oxide from silica upon calcination [37,41,42]. If rhenium mobility is already observed in Re_2O_7/Al_2O_3 [26] it is expected to be much higher on silica, which might well account for the significant volatilization of rhenium during catalytic experiments.

Products observed from methane oxidation are CO, HCHO and CO_2. Additionally, C_2H_n hydrocarbons are also observed on the 0.8 V catalyst. Fig. 5 shows methane conversion as a function of reaction temperature. Reactivity of the silica support is also included for comparative purposes. All catalysts, except 0.05 Re, are stable during the time of reaction. 0.05 Re deactivates during approximately the first 12 h of reaction (Fig. 6). Vanadia/silica catalyst activity is constant, even when part of the vanadia is lost during catalytic experiments. It is likely that only aggregated vanadium oxide species could be lost from the catalyst since they could melt at reaction temperature. Furthermore, aggregated vanadium oxide is much less reactive than dispersed surface vanadium oxide. The reactivity trend follows the sequence 0.8 V > 0.8 Mo > 0.8 W > 0.05 Re > SiO_2. Due to the significant deactivation of rhenium, Table 2 compiles methane conversion values at 883 K for all catalysts and the silica support. The values for the 0.05 Re catalyst correspond to its initial stages when little deactivation has taken place. TOF-numbers have also been calculated assuming that all supported metal oxide phases are active in the reaction. The activity of the silica support has been subtracted prior to the TOF number calculation. These results clearly emphasise the high specific activity of rhenium sites for methane conversion. Rhenium-based catalysts have also proved to be highly active in different catalytic reactions [26–29].

Selectivity to different products vs. methane conversion trends are presented in Fig. 7. The values for the 0.05 Re catalyst correspond to the stabilized catalyst (about 20 h on stream). Some general trends are observed for all catalysts. Selectivity to formaldehyde decreases with conversion, and selectivity to CO increases. The complementary trend between these two species is more evident for 0.8 V, 0.8 Mo, and 0.8 W catalysts. This is consistent with CO being a secondary product originating from decomposition of HCHO. Selectivity to CO_2 does not approach zero at zero methane conversion. This

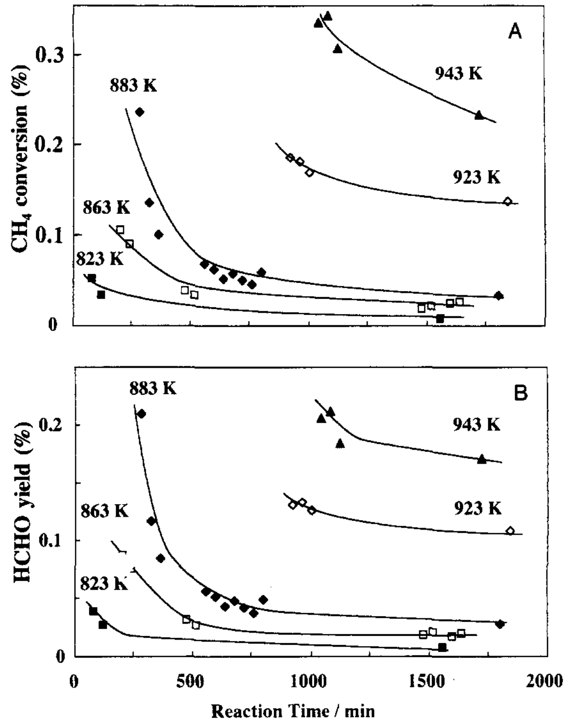

Fig. 6. Methane conversion (A) and yield to formaldehyde (B) on 0.05 Re vs. time on-stream. Reaction conditions: $CH_4/O_2 = 2$ molar; $W/F = 2$ g h mol^{-1}; $W = 50$ mg.

indicates that it is likely that carbon dioxide is a primary product. CO selectivity tends to stabilize with conversion of methane to different values which follow the trend 0.8 V > 0.8 Mo > 0.8 W > 0.05 Re ~ SiO_2. The presence of C_2H_n hydrocarbons is not observed on 0.8 V. Selectivity to C_2H_n (essentially ethane) products appears to follow the opposed trend to CO selectivity. The C_2H_n/CO selectivity ratio is presented in Fig. 8. The C_2H_n/CO selectivity ratio is quite similar for 0.8 Mo and 0.8 W catalysts, but is highest for the 0.05 Re catalyst, specially at low reaction temperature (below ca. 920 K) where no CO could be detected. It appears that the partial oxidation of methane reaction on these catalysts may proceed via non-oxygenated intermediates, its importance being determined by the specific supported oxide.

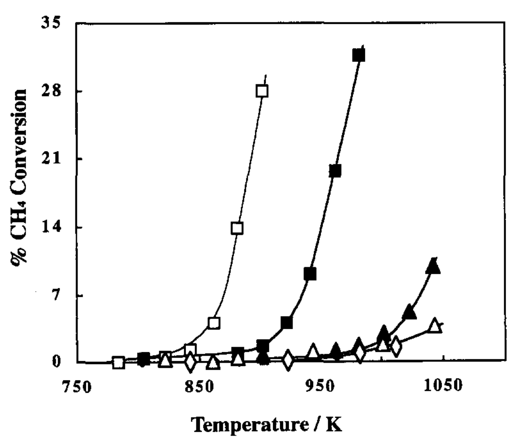

Fig. 5. (A) Methane conversion vs. reaction temperature: (□) 0.8 V; (■) 0.8 Mo; (▲) 0.8 W; (△) 0.05 Re; and (◇) SiO_2. Reaction conditions: $CH_4/O_2 = 2$ molar; $W/F = 2$ g h mol^{-1}; $W = 50$ mg.

We previously reported the formation of C_{2+} hydrocarbons on very low surface area vana-

Table 2
Methane conversion on silica-supported oxide catalysts [a]

Catalyst	CH_4 conversion (mol%)	TOF×10^3 (s^{-1}) [b]
0.8 V [c]	13.9	73
0.8 Mo	0.6	3
0.8 W	0.1	0.1
0.05 Re [d]	0.23	12
SiO_2	0.08	

[a] Reaction conditions: 883 K; $CH_4/O_2 = 2$ molar; $W/F = 2$ g h/mol.
[b] TOF number has been calculated subtracting the activity from silica support.
[c] TOF number for 0.8 V has been calculated on the vanadium loading determined by XPS after catalytic experiments.
[d] Values for 0.05 Re correspond to fresh catalyst prior to loss of active phase.

dium oxide-based catalysts [21]. In order to evaluate the possible presence of non-oxygenated intermediates on the 0.8 V catalyst, in situ DRIFTS and TPD-MS experiments were performed. The catalyst was previously impregnated with a solution of formaldehyde in water and methanol. DRIFTS spectra are presented in Fig. 9. Molecular oxygen was flowing through the DRIFTS cell while temperature was raised stepwise. IR bands of adsorbed HCHO are observed at room temperature on a hydrated sample. As temperature is increased the sample dehydrates and methane evolves from the 0.8 V catalyst. No adsorbed hydrocarbon remains on the surface at higher temperatures. Indeed no

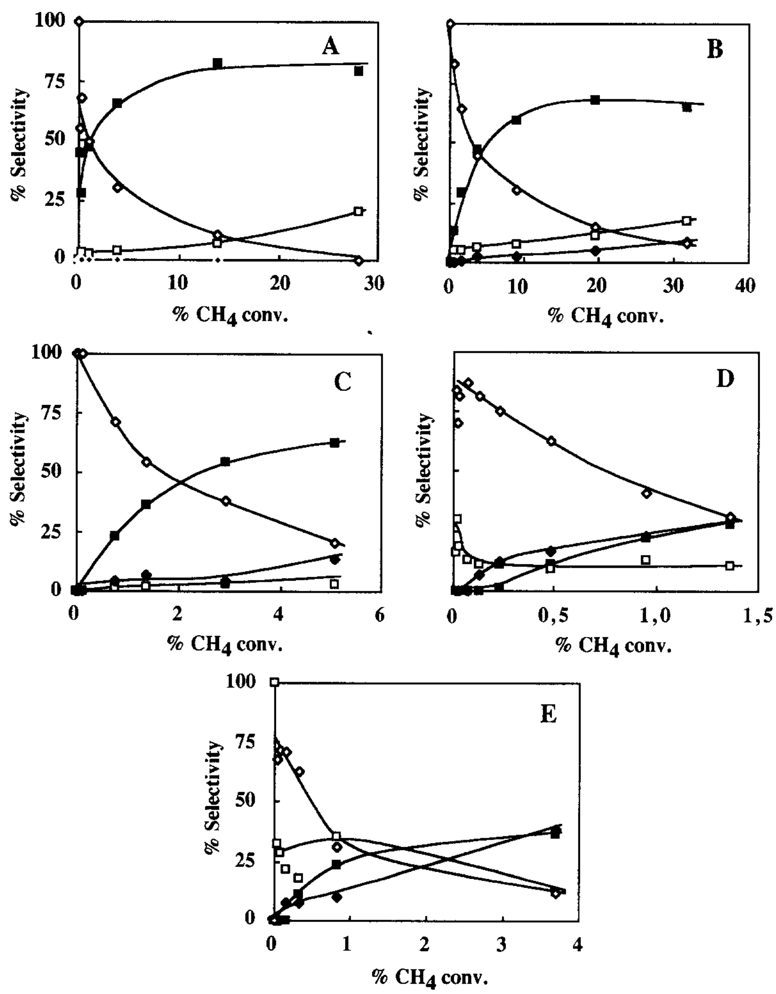

Fig. 7. Selectivity vs. conversion plots for the different catalysts and silica-support: (■) CO; (□) CO_2; (◇) HCHO; (◆) C_2H_n. (A) 0.8 V; (B) 0.8 Mo; (C) 0.8 W; (D) 0.05 Re; (E) SiO_2. Reaction conditions as in Fig. 5.

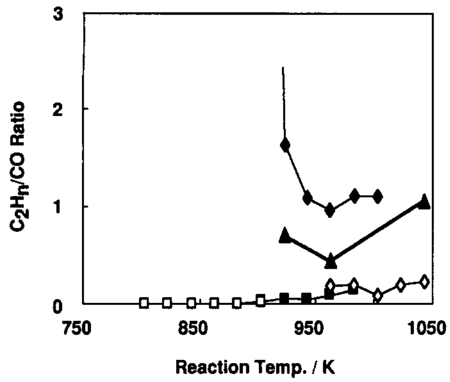

Fig. 8. C_2H_n/CO selectivity ratio vs. reaction temperature: (■) 0.8 Mo; (□) 0.8 V; (♦) 0.025 Re; (◇) 0.8 W; (▲) SiO_2. Reaction conditions as in Fig. 5.

oxygenated species are generated from adsorbed formaldehyde on the vanadium oxide containing catalyst in flowing oxygen. A temperature programmed reaction-mass spectrometry experiment (Fig. 10) was performed with a sample prepared like the one for the DRIFTS experiment. Heating of the sample yields evolution of methanol and formaldehyde with maxima at ca. 410 and 770 K, respectively. Evolution of methane (m/e 16 > 15 > 14) in similar amounts to that of HCHO is observed at temperatures

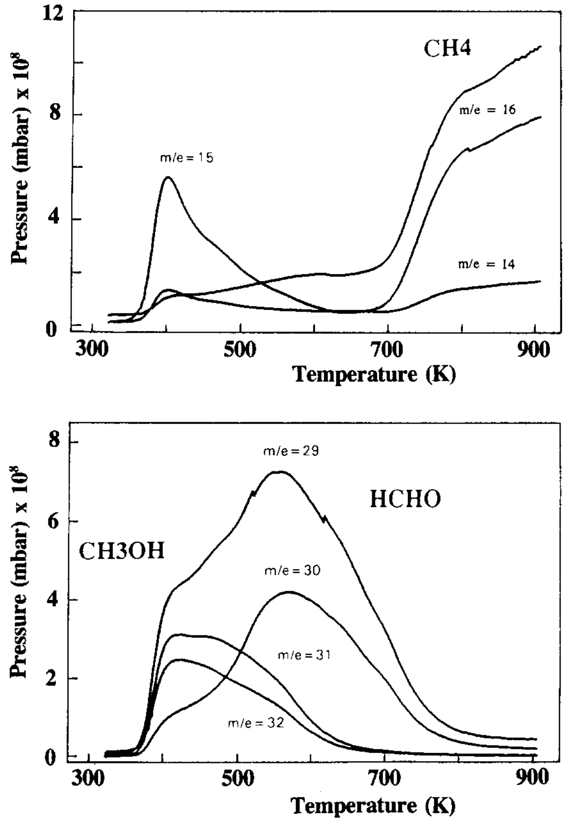

Fig. 10. Temperature programmed reaction-mass spectrometry of 0.8 V sample impregnated with formaldehyde, water and methanol.

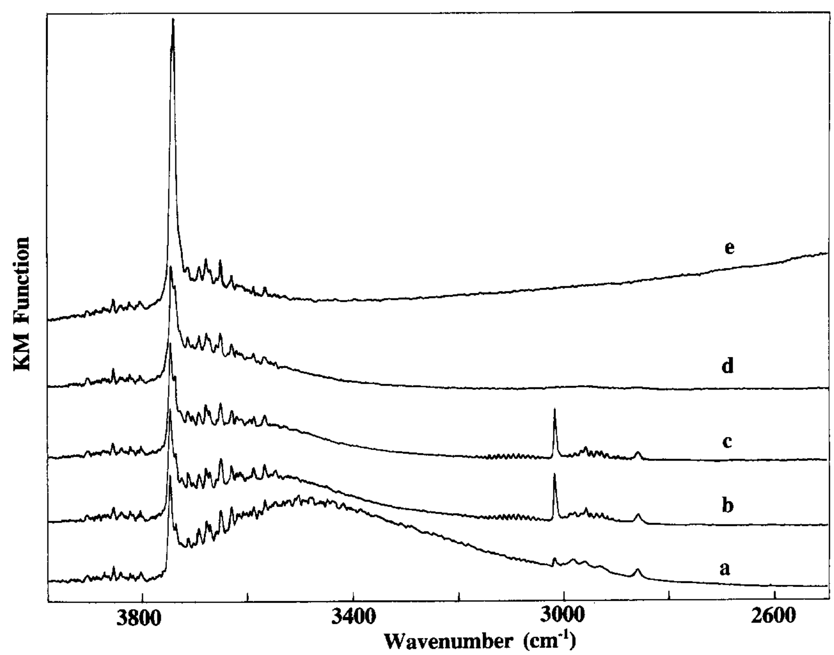

Fig. 9. In situ DRIFTS spectra on 0.8 V in flowing oxygen at different temperatures: (a) 298 K; (b) 373 K; (c) 473; (d) 673 K; (e) 873 K.

above 770 K, supporting the formation of non-oxygenated products from oxygenated adsorbed species. The peaks observed at low temperatures, mainly at $m/e = 15$, do not originate from methane since $m/e = 16$ is not the most intense fragment. Blank experiments on a fresh 0.8 V catalyst show a maximum for the m/e 15 signal at the same temperature as for a 0.8 V catalyst impregnated with HCHO, CH_3OH and water. These low temperature peaks must originate from ambient adsorbed species.

4. Discussion

Relative activity for methane conversion on the studied oxides follows the trend V > Mo > W > > Re. This trend appears to be associated with the reducibility of the catalyst observed in the TPR experiments reported here. However some of us previously showed that methane conversion does not correlate with catalyst reducibility [25]. But the reducibility may determine how reduced the catalyst will be during the reaction conditions. In situ Raman spectroscopy shows that silica-supported vanadium oxide is slightly reduced during catalytic experiments [14] (ca. 10% of vanadium sites) [43]. This is not the case for silica-supported molybdenum oxide catalysts under the same experimental conditions [25] where no appreciable reduction can be observed. We do not expect it to be the case for 0.8 W catalyst either, as TPR experiments suggest. The presence of partially reduced vanadium oxide species will provide sites for adsorption of oxygen thus increasing reactivity. Selectivity to CO approaches a similar value for 0.8 Mo and 0.8 W catalysts, in addition the C_2H_n/CO selectivity ratio is essentially the same for these two catalysts. All of this suggests that reaction must proceed in quite a similar way for 0.8 Mo and 0.8 W catalysts. The difference in reactivity between these two catalysts must originate from the high resistance of supported tungsta to reduction. This will decrease the number of sites which can activate oxygen, and therefore activate methane. Even when no reduction of molybdenum oxide is observed by in situ Raman spectroscopy [25], some slight extent of reduction might be expected which will be more than on tungsten oxide.

The role of the oxide is indeed important in the activation of methane [21] but it is not the only means to activate methane. $O_2 + CH_4$ reaction forms radicals thus initiating the reaction. This reaction may occur in the homogenous phase and may be promoted by the high surface area silica support and is clearly promoted by supported oxides [21]. As already reported by Hodnett et al. [10] for silica-supported vanadium oxide catalysts, methane activation can occur through oxygen activation on the supported oxide. The interaction of oxygen with the catalyst activates oxygen making it more reactive thus promoting methane activation. However, the high surface area of the support can also promote further non selective oxidation of intermediates by increasing their contact with the catalyst [21]. This negative effect could be minimized by decreasing the surface area of the support. Elimination of support area decreases CO by 50% and increases partial oxidation products such as formaldehyde, methanol, and C_{2+} hydrocarbons [21].

From the results presented here, it does appear that for a specific surface area of the support, the use of the appropriate supported oxide improves selectivity to partial oxidation products (C_2H_n) vs. non selective CO. Results reported here (activity, in situ DRIFTS and TPD-MS) suggest a reaction mechanism in which both non-oxygenated and oxygenated intermediates are present and which is illustrated in Scheme 1.

Methane can be converted into radicals by reaction with oxygen in the gas phase or in the presence of the catalyst. The radicals may react in the gas phase and on the catalyst. In the present paper, gas-phase reactions are minimized and catalytic performance will be determined by the catalyst alone. The distribution of

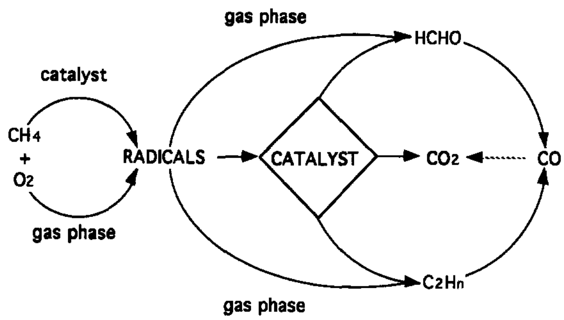

Scheme 1.

product between HCHO and CO appears to be a function of methane conversion, which in turn is determined by methane residence time and reaction temperature. Meanwhile, the ratio of C_2H_n to oxygen containing products is determined by the supported oxide. Production of non-oxygenated intermediates may take place in all supported oxides, however the high reactivity of vanadium oxide converts partial oxidation intermediates to CO. Rhenium catalysts have a remarkable selectivity for production of C_2H_n hydrocarbons over CO compared with other metal oxides in the series. Further research is currently being conducted on rhenium catalysts.

5. Conclusion

Methane can be partially oxidized on all of the silica-supported oxides studied (V, Mo, W, and Re). Formaldehyde, C_2H_n, and CO_2 are primary products obtained in this reaction, meanwhile at least some of the CO originates from further oxidation of formaldehyde and hydrocarbons. Supported vanadium oxide is the most reactive catalyst, perhaps due to its higher reducibility which would rapidly turnover sites for oxygen activation. Rhenium oxide has an elevated selectivity. Unfortunately, it is not stable during reaction conditions. Chemical routes to stabilize rhenium should be found to take advantage of its catalytic performance. Catalytic activation of oxygen leads to activation of methane thus increasing reactivity. Distribution of products between formaldehyde and CO appears to depend on the supported oxide and on methane conversion. The conversion of partial oxidation intermediates to C_2H_n or CO is largely determined by the supported oxide for a given specific surface area.

Acknowledgements

Financial support of this work by the Commission of the European Union (grant JOU2-CT92-0040) and CICYT (grant MAT95-0894) are gratefully acknowledged.

References

[1] J.H. Lunsford, Catal. Today, 6 (1990) 235.
[2] N.D. Spencer, J. Catal., 109 (1988) 187.
[3] M.A. Bañares and J.L.G. Fierro, Catal. Lett., 17 (1993) 205.
[4] A. Parmaliana, F. Arena, F. Fusteri, D. Miceli and V. Sokolovski, Catal. Today, 24 (1995) 231.
[5] T.R. Baldwin, R. Burch, G.D. Squire and S.C. Tsang, Appl. Catal., 74 (1991) 137.
[6] J.C. Mackie, Catal. Rev.-Sci. Eng., 33 (1991) 169.
[7] R. Pitchai and K. Klier, Catal. Rev.-Sci. Eng., 28 (1986) 13.
[8] H.D. Gesser, N.R. Hunter and C.B. Prakash, Chem. Rev., 85 (1985) 235.
[9] M.A. Bañares, I. Rodríguez-Ramos, A. Guerrero Ruíz and J.L.G. Fierro, in L. Guczi, F. Solymosi and P. Tetenyi, Editors, New Frontiers in Catalysis, Vol. B, Elsevier, Amsterdam, 1993, p. 1131.
[10] B. Kartheuser, K.B. Hodnett, H. Zanthoff and M. Baerns, Catal. Lett., 21 (1993) 209.
[11] M.M. Koranne, J.G. Goodwin, Jr. and G. Marcelin, J. Phys. Chem., 97 (1993) 673.
[12] R. Mauti and C.A. Mims, Catal. Lett., 21 (1993) 201.
[13] Y. Barbaux, A.R. Elamrani, E. Payen, L. Gengembre, J.P. Bonelle and B. Gryzbowska, Appl. Catal., 44 (1988) 117.
[14] M.M. Koranne, J.G. Goodwin, Jr. and G. Marcelin, J. Catal., 148 (1994) 378.
[15] M. Faraldos, M.A. Bañares, J.A. Anderson, H. Hu, I.E. Wachs and J.L.G. Fierro, J. Catal., in press.
[16] K. Otsuka and M. Hatano, J. Catal., 108 (1987) 252.
[17] V. Amir-Ebrahimi and J. Rooney, J. Mol. Catal., 50 (1989) L17.
[18] T. Weng and E.E. Wolf, Appl. Catal. A, 96 (1993) 383.
[19] M. López Granados and E.E. Wolf, Appl. Catal. A, 131 (1995) 263.
[20] M.A. Bañares, J.L.G. Fierro and J.B. Moffat, J. Catal., 142 (1993) 406.

[21] F. Martín-Jiménez, J.M. Blasco, L.J. Alemany, M.A. Bañares, M. Faraldos, M.A. Peña and J.L.G. Fierro, Catal. Lett., 33 (1995) 279.
[22] S. Irusta, L.M. Cornaglia, E.E. Miró and E.A. Lombardo, J. Catal., 156 (1995) 167.
[23] Q. Sun, J.I. Di Cosimo, R.G. Hermann, K. Klier and M.M. Bhasin, Catal. Lett., 15 (1992) 371.
[24] C.C. Williams, J.G. Ekerdt, J.-M. Jehng, F.D. Hardcastle, A.M. Turek and I.E. Wachs, J. Phys. Chem., 95 (1991) 8781.
[25] M.A. Bañares, N.D. Spencer, M.D. Jones and I.E. Wachs, J. Catal., 146 (1994) 204.
[26] R. Spronk, J.A.R. van Veen and J.C. Mil, J. Catal., 144 (1993) 472.
[27] I.E. Wachs, G. Deo, A. Andreini, M.A. Vuurman and M. de Boer, submitted.
[28] P. Chaumont and C.S. John, J. Mol. Catal., 46 (1988) 317.
[29] P. Amigues, Y. Chauvin, D. Commereuc, C.C. Lai, Y.H. Lui and J.M. Pan, Hydrocarbon Process., October (1990) 79.
[30] F.D. Hardcastle, I.E. Wachs, J.A. Horsley, G.H. Via, J. Mol. Catal., 46 (1988) 15.
[31] D.S. Kim and I.E. Wachs, J. Catal., 141 (1995) 419.
[32] D.A. Shirley, Phys. Rev., 35 (1972) 4909.
[33] D.S. Kim, M. Ostromecki, I.E. Wachs, S.D. Kohler and J.G. Ekerdt, Catal. Lett., 33 (1995) 209.
[34] M. Faraldos, J.A. Anderson, M.A. Bañares, J.L.G. Fierro and S.W. Weller, submitted.
[35] N. Das, H. Eckerdt, H. Hu, I.E. Wachs, J.F. Walzer and F.K. Feher, J. Phys. Chem., 97 (1993) 8240.
[36] N.N. Greenwood, The Chemistry of the Elements, Pergamon Press, 1987.
[37] M. Sibeijn and J.C. Mol, J. Mol. Catal., 67 (1991) 279.
[38] X. Xiaoding, C. Boelhouer, J.I. Benecke, D. Vonk and J.C. Mil, J. Chem. Soc., Faraday Trans. 1, 82 (1986) 1945.
[39] J. Leyrer, D. Mey and H. Knözinger, J. Catal., 124 (1990) 349.
[40] S.R. Stampfl, Y. Chen, J.A. Dumesic, N. Chumming and C.G. Hill, J. Catal., 105 (1987) 445.
[41] J.-M. Jehng and I.E. Wachs, Catal. Lett., 13 (1992) 9.
[42] J.-M. Jehng, I.E. Wachs, B.M. Weckhuysen and R.A. Schoonheydt, J. Chem. Soc., Faraday Trans., 91 (1995) 953.
[43] Q. Sun, J.-M. Jehng, H. Hu, R.G. Herman, I.E. Wachs and K. Klier, 207th ACS Meeting, San Diego, CA, 1994.